Quaternary Science Reviews

1   **Title:** The influence of climatic change, fire and species invasion on a southern temperate

2   rainforest system over the past 18, 000 years.

3

4   **Running title:** Temperate rainforest response to climate and fire.

5

6   Fletcher, Michael-Shawn[1*]

7   Bowman, David MJS[2]

8   Whitlock, Cathy[3,4]

9   Mariani, Michela[1,5]

10   Beck, Kristen K[1,6]

11   Stahle, Laura N[3]

12   Hopf, Felicitas[7]

13   Benson, Alexa[1]

14   Hall, Tegan[1]

15   Heijnis, Hendrik[8]

16   Zawadzki, Atun[8]

17

18   [1]School of Geography, University of Melbourne, 221 Bouverie Street, Carlton, Victoria,

19   3053

20   [2]School of Plant Science, University of Tasmania, Hobart, TAS, Australia 7001

21   [3]Department of Earth Sciences, Montana State University, Bozeman, MT, 59717 USA

22   [4]Montana Institute on Ecosystems, Montana State University, Bozeman, MT, 59717 USA

23   [5]School of Geography, University of Nottingham, Nottingham, UK

24   [6]School of Geography, University of Lincoln, Lincoln, LN6 7TS, UK

25   [7]Archaeology and Natural History, College of Asia and the Pacific, The Australian

26   National University, Canberra, ACT 0200, Australia

27   [8]Australian Nuclear Science and Technology Organisation, Locked Bag 2001, Kirrawee

28   DC NSW, Australia 2232

29   *corresponding author

30

35

36 **Abstract**

37 We aim to understand how did cool temperate rainforest respond to changes in climate and

38 fire activity over the past 18 kcal yrs, interrogating the role that flammable plant species

39 (such as *Eucalyptus*) have in the long-term dynamics of rainforest vegetation. We used

40 high-resolution pollen and charcoal analysis, radiometric dating (lead and carbon), modern

41 pollen-vegetation relationships, detrended correspondence analysis, rarefaction

42 (palynological richness), rate of change and granger causality to understand the patterns

43 and drivers of change in cool temperate rainforest from the sediments of Lake Vera,

44 southwest Tasmania through time. We record clear changes in key rainforest taxa in

45 response to climatic change throughout the record. The spread of rainforest through the

46 lake catchment in the early and mid-Holocene effectively negated disturbance from fire

47 despite a region-wide peak in fire activity. An anomalously dry period in the late-Holocene

48 resulted in a local fire that facilitated the establishment of *Eucalyptus* within the local

49 catchment. Granger causality tests reveal a significant lead of *Eucalyptus* over fire activity

50 in the Holocene, indicating that fires were enhanced by this pyrogenic taxon following

51 establishment.

52

55

56

57   **1. Introduction**

58   Climate change represents a significant and long-term stress on biological systems, which

59   is exacerbated by the occurrence of extreme events, such as heatwaves, droughts and

60   wildfires (Harris et al. 2018). For example, wildfires are predicted to increase in many

61   regions in response to climate change (Moritz et al. 2012), compounding the ongoing

62   effects of climate change on the growth, reproduction and recovery of plant species and

63   potentially resulting in fire-driven ecosystem collapse (Bowman et al. 2014; Enright et al.

64   2015). Moreover, the spread of fast growing and highly flammable plant species, such as

65   *Eucalyptus*, by people across the Earth threatens to further increase the probability of fire

66   (Fletcher et al. 2020). Indeed, the potential of this threat has motivated a ban on Eucalypt

67   plantations in some regions. There is, thus, an urgent need for data on the role of flammable

68   species invasion in driving fire regime change if we are to effectively manage fire sensitive

69   vegetation into the future.

70

71   The analysis of long-term rainforest dynamics in Tasmania, Australia, represents an ideal

72   case study for this important problem. The rainforests in this topographically complex

73   region persist in tiny topographic fire refugia in a landscape dominated by flammable

74   vegetation (Wood et al. 2011). The modern dominance of the landscape by flammable

75   vegetation was established during the Last Glacial-Interglacial Transition (LGIT) in

76   response to landscape burning by the Palawa People of Tasmania (Fletcher & Thomas

77   2010), the Indigenous owners of this mountainous temperate island. Following the invasion

78   by the British, there has been a marked increase in the occurrence of catastrophic wildfire

79   in this landscape (Marsden-Smedley 1998; Mariani & Fletcher 2016) which has decimated

80   huge swathes of pyrophobic rainforest (Cullen 1987; Cullen & Kirkpatrick 1988b, a; Holz

81   et al. 2015; Holz et al. 2020), presumably due to the shift in the way fire was applied in the

82   landscape and the removal of a sophisticated cultural burning methodology that had a net

83   result of maintaining lower landscape fuel loads (McKemey et al. 2020).

84

85   The precariousness of topographic fire refugia in Tasmania in a landscape of increasing

86   fire activity and in a rapidly changing climate has prompted suggestions that the extinction

87   of these very long lived (some tree species live in excess of 2000 years) and hyper fire-

88   sensitive Gondwanan relicts is all but a *fait accompli* (Rickards 2016). While recent work

89   on high altitude rainforest communities in Tasmania demonstrates that both climate change

90   (Mariani et al. 2019) and *Eucalyptus* invasion (Fletcher et al. 2020) can both facilitate

91   localised fire-driven elimination of rainforest, little is known about the response of lowland

92   rainforest to these pressures. Here, we use a detailed palaeoecological analysis of lake

93   sediments from within a catchment currently occupied by both fire-sensitive temperate

94   rainforest and *Eucalyptus* forest to elucidate the response of this vegetation type to changes

95   in climate, fire and species composition over the last 18,000 years (18 kcal yrs) in

96   southwest Tasmania, Australia.

97

98   Several factors mediate the local impact of fire on vegetation, such as macro- and

99   microclimate, topography, species composition, the presence of fire-breaks and human

100   intervention. Rainforest in Tasmania is largely restricted to steep south-facing slopes,

101   where a combination of microclimate, topographic fire-breaks, low fuel flammability and

102   increased sub-canopy humidity form an effective barrier to the spread of fire carried readily

103   across the landscape by flammable plant species (Wood et al. 2011; Cadd et al. 2019).

104   Indeed, fires only occur in Tasmanian rainforest following anomalously low summer

105   rainfall, which allows sufficient drying of fuel loads to support fire (Styger & Kirkpatrick

106   2015). Data from single fire events within rainforest indicates that post-fire rainforest

107   regeneration does occur in the absence of repeated burning, while post-fire invasion by

108   flammable plant species (Hill & Read 1984), such as *Eucalyptus*, after repeated fires can

109   alter the post-fire species mix (Fletcher et al. 2014; Fletcher et al. 2020). The change in

110   vegetation that accompanies an increase in pyrogenic species results in more flammable

111   fuel load that can facilitate a change in fire regime, potentially leading to the localised loss

112   of rainforest vegetation (Fletcher et al. 2014; Fletcher et al. 2018b; Fletcher et al. 2020).

113

114   While the role of species invasion in changing local ecosystem dynamics and facilitating

115   an ecosystem shift is well recognised (Wilson & Agnew 1992), relatively little is known

116   about the potential of highly flammable and fire-adapted *Eucalyptus* species to change local

117   fire regimes and eliminate rainforest vegetation. Detailed long-term (palaeoecological)

118   analysis of vegetation and fire in high altitude Tasmanian rainforest indicates that a

119   replacement of rainforest by eucalypt-dominant vegetation can occur following repeated

120   millennial-scale fires, supporting the contention that an invasion by fire-promoting species

121   can lead to a change in local fire regime and the localised extinction of rainforest vegetation

122   (Fletcher et al. 2014; Fletcher et al. 2020). The Fletcher et al. (2014, 2020) studies appear

123   to be consistent with models of the evolution of flammability that depict the destruction of

124   competitors via self-immolation (Bond & Midgley 1995), demonstrating that fire and

125   climate alone are insufficient to drive transitions between alternative vegetation states in

126   the absence of flammable plants like *Eucalyptus* which act as ecosystem engineers

127   (Fletcher et al. 2020).

128

129   We use high-resolution pollen and charcoal analyses to reconstruct vegetation and fire

130   dynamics over the last 18 kcal from Lake Vera (42°16'25.03"S, 145°52'52.70"E, 570 masl)

131   in southwest Tasmania, Australia, service the following aims: 1- to investigate how

132   lowland rainforest in Tasmania responded to the well-described changes in climate and fire

133   activity over the past 18,000 years (18 kcal); and 2- to test whether *Eucalyptus* also act as

134   an ecosystem engineer in this system, as observed in higher altitude rainforest in Tasmania.

135

136

137   **2. Study region**

138   Tasmania (41-44° S) is a cool temperate continental island that is bisected by northwest-

139   to-southeast trending mountain ridges which intercept mid-latitude westerly winds and

140   result in a steep orographic precipitation gradient across the island (decreasing west-to-

141   east). The temperature regime of Tasmania's southwest is cool (5-7° C June to August; 14-

142   16° C December to February), and precipitation exceeds evaporation for most of the year

143   (Sturman & Tapper 2006). The southwest region is underlain by low-nutrient-yielding

144   quartz-dominated metasediments and occasional outcrops of rock types with higher

145   nutrient potential, such as dolerite and limestone (Jackson 1999). The cool, wet climate and

146   infertile soils result in slow rates of vegetation change in southwest Tasmania. A long

147   history of human occupation (ca. 40 kcal BP) (Cosgrove 1999)and anthropogenic burning

148   has also left an enduring imprint on the regional vegetation (Fletcher & Thomas 2010),

149   which is dominated by open pyrophytic vegetation types and highly flammable *Eucalyptus*-

150   forests (sclerophyll forest).

151

152   While past ignition sources were a combination of human and lightning, centennial- to

153   millennial-scale trends in fire activity in this high-biomass landscape are modulated by

154   climate (Mariani & Fletcher 2016; Mariani & Fletcher 2017). A recent synthesis of changes

155   in biomass burning over the last 12 kcal from across the west of Tasmania has revealed a

156   tight coupling between long-term fire activity and hemispheric-scale hydroclimatic change

157   (Mariani & Fletcher 2017), with a step-wise increase in fire activity across the region

158   between 3-4 kcal BP responsible for a region-wide decrease in rainforest cover – possibly

159   associated with ENSO-driven changes in rainfall variability) (Beck et al. 2017; Mariani et

160   al. 2017; Mariani & Fletcher 2017; Stahle et al. 2017; Mariani et al. 2019).

161

162   This study focuses on Lake Vera, a small glaciated lake with a small narrow catchment

163   (0.17 km²) that is oriented SW-NE with a surface area of 0.15 km² approximately 4.5 km

164   northeast of Frenchman's Cap (1443 masl). The catchment is a steep-sided glacial trough

165   valley dominated by both coniferous rainforest vegetation and *Eucalyptus*-dominant forest

166   on the Frenchman's Cap massif, an isolated, precipitous mountain of quartzite rock, located

167   40 km inland of the west coast (Fig. 1). In this region, average annual rainfall extracted

168   from   gridded   climate   data   is   *ca.*   2700   mm   p/a

169   (http://www.bom.gov.au/climate/averages/climatology/gridded-data-info/gridded-

170   climate-data.shtml), with a dominant westerly airflow through most of the year. The

171   climatic potential vegetation in the absence of fire is cool temperate rainforest on all

172 geological types. Actual vegetation patterns and dynamics in the landscape are governed

173 by an interaction between disturbance from fire and a range of biophysical factors, such as

174 elevation, aspect, geology, soils and species composition.

175

176 Alpine taxa are present above ca. 900 masl and are characterised by both fire-sensitive and

177 fire tolerant/promoted communities. Poorly drained plains and exposed northwest-facing

178 slopes encourage the expansion of treeless pyrogenic vegetation (moorlands) dominated

179 by a mix of shrubs (*Melaleuca, Leptospermum*) and graminoids (Restionaceae and

180 Cyperaceae), particularly the robust sedge *Gymnoschoenus sphaerocephalus*. Flammable

181 wet sclerophyll forests dominated by *Eucalyptus* and an array of understorey rainforest

182 species form in areas of moderate fire frequency (*ca.*70-400 year fire-return intervals)

183 (Jackson 1968), usually on northwest-facing slopes where greater solar radiation exposure

184 leads to drier fuel loads (Wood et al. 2011). Within these wet sclerophyll forests,

185 *Eucalyptus* species act as system 'engineers', promoting higher fire frequencies with

186 flammable plant tissues and fire-tolerant/dependent reproduction strategies, and by

187 increasing forest-floor tinder and decreasing sub-canopy humidity (Bowman 2000; Brooks

188 et al. 2004).

189

190 Rainforest dominated by *Nothofagus cunninghamii*, *Phyllocladus aspleniifolius*,

191 *Eucryphia lucida*, *Atherosperma moschatum* and *Andopetalum biglandulosum* is restricted

192 to the mid-slopes of mountains and deep/steep ravines that afford topographic protection

193 from fire (Wood et al. 2011). These systems are poorly adapted to fire as the limited seed

194 dispersal and slow maturation rates of many canopy species within these forests

195 (Kirkpatrick & Dickinson 1984; Cullen 1991) render them vulnerable to local extinction

196 when fire frequencies increase (Fletcher et al. 2014; Fletcher et al. 2018b; Fletcher et al.

197 2020). High altitude (montane) rainforest forms at higher elevations up to the timberline

198 and species include *Athrotaxis cupressoides*, *A. selaginoides* (Cupressaceae) and

199 *Nothofagus gunnii* (Harris & Kitchener 2005). All these vegetation types are present in the

200 Lake Vera catchment (Fig. 1): the largest portion of the catchment is comprised of steep

201 (0.3-0.6 gradient), sheltered, southeast-facing slopes covered by rainforest, while a smaller

202 steep (0.4-0.7 gradient) northwest-facing slope supports *Eucalyptus*-dominated wet

203 sclerophyll forest, suggesting more frequent disturbance from fire on the relatively drier

204 (i.e. more sun-exposed) NW-facing slopes. The north-eastern margin of the lake is

205 occupied by pyrogenic *Gymnoschoenus sphaerocephalus* moorland and heath complexes,

206 a highly flammable vegetation type that dominates the broader landscape of south and

207 western Tasmania.

208

209 **3. Methods**

210 *3.1 Core Collection and Sampling*

211 A 105.5-cm-long core (TAS1108SC1) was taken from the centremost point of the lake

212 (49.5 m depth) using a 6-cm-diameter polycarbonate tube attached to a Universal Corer in

213 2011. Recovery included the mud-water interface. A Livingstone corer was used to retrieve

214 sediments from a 12 m-deep submerged bench northeast of the short core site, 3.2 m of

215 sediment was recovered in 1 m continuous sections (TAS1108LCA) in 2011 (Fig. 1).

216 TAS1108SC1 was sub-sampled at 0.5-cm intervals and TAS1108LCA was sub-sampled at

217 1-cm intervals in the laboratory. Fig. 1 shows the locations of the cores and of an earlier

218   core taken from Lake Vera by Macphail (1979). A second 6-m core (TAS1508N1) from

219   the deepest part of the basin was retrieved in 2016 that, while failing to penetrate to the

220   base of the lake sediment unit, allows for comparison with the existing core TAS1108LCA

221   to assess the influence of core location over the pollen stratigraphy. The results of this

222   comparison are presented in Fig. S1 of the Supporting information (Appendix S1).

223

224   *3.2 Chronology*

225   A total of six samples were analysed for ^{210}Pb analysis using alpha spectrometry at the

226   Australian National Science and Technology Organisation (ANSTO) and 11 bulk-sediment

227   radiocarbon samples were submitted to the Woods Hole NOSAMS AMS facility for

228   radiocarbon dating (Table 2). All samples were bulk sediment and radiocarbon ages were

229   calibrated using the Southern Hemisphere radiocarbon calibration dataset SHCal20 (Hogg

230   et al. 2020) (Table S1; Appendix S2). Age-depth modelling was performed in *clam v2.2*

231   (Blaauw 2010) using a locally smoothed (0.2) spline regression (Fig. 2). A further 17

232   radiocarbon ages were obtained from TAS1508N1 (all performed on macrofossils) and the

233   position of these dates is indicated in Fig. 2 .

234

235   *3.3 Charcoal analysis and core correlation*

236   Macroscopic charcoal analysis was performed on 2-cm^3 volume samples taken at

237   continuous 5-mm (for TAS1108SC) and 1-cm (for TAS1108LCA) intervals following the

238   method described in Whitlock and Larsen (2001). Charcoal accumulation rates (CHAR;

239   particles cm^{-2} yr^{-1}) were calculated using the results of the age-depth modelling. The tie-

240   point between TAS1108SC and TAS1108LCA was determined using the independently

241   dated CHAR records of each core (Fig. S2; Appendix S2). Sediment focussing to the

242   deepest point of the lake basin resulted in substantially higher delivery of charcoal to

243   TAS1108SC than TAS1108LCA (Fig. S2; Appendix S2) and we corrected the values via

244   multiplication with a factorial division to synthesise the two CHAR records: i.e. we divided

245   the CHAR values in the overlapping sections (TAS1108SC1/TAS1108LCA) to estimate

246   the degree of increased charcoal deposition in the lake's depositional centre relative to the

247   shallower coring location. This 'factor' was then used to correct the values from

248   TAS1108SC1 to allow stitching of these two sequences. We focus our interpretations on

249   relative changes in the CHAR sequence, not absolute CHAR values, thus, while

250   acknowledging the alteration to the primary data, we contend that the resulting 'synthetic'

251   CHAR sequence is suited to the aims of this study. Following this, we applied a regime

252   shift index (RSI) algorithm to our composite CHAR record (sensu Morris et al. 2013),

253   incorporating a sequential Student's t-test (Huber's WF=5, P<0.0001, cut-off=500 yrs) to

254   determine statistically significant shifts in mean values of two subsequent charcoal (i.e.

255   fire) regimes (Rodionov 2004; http://www.beringclimate.noaa.gov/regimes/).

256

257   *3.4 Palynology and data analysis*

258   A total of 213 samples were analysed for pollen analysis using standard procedures (Faegri

259   & Iversen 1989). Pollen enumeration targeted 300 terrestrial grains, with final counts

260   ranging from 298-378. The terrestrial pollen data are expressed as percentages of the

261   terrestrial pollen sum (TP). Fern spores are presented as percentages of a sum inclusive of

262   TP and fern spores, while wetland and aquatic percent values are calculated from a sum of

263   all pollen and spores. Pollen zones were identified using the aid of a stratigraphically

264   constrained cluster analysis (CONISS) on the TP dataset (Grimm 1987), with the number

265   of zones and subzones identified using broken-stick modelling performed in the *rioja*

266   package v 0.9.21 in *R* (Juggins 2012).

267

268   We conducted an unconstrained ordination analysis (Detrended Correspondence Analysis

269   - DCA) to identify the main compositional trends through time. The DCA was performed

270   on the terrestrial fossil pollen dataset and the main axis of variation (DCA Axis 1) was

271   extracted as an indicator of the dominant trends in the terrestrial pollen dataset through

272   time. To allow mapping of the fossil pollen data to terrestrial vegetation, a second DCA

273   was performed on a combination of the Lake Vera fossil pollen dataset and a modern pollen

274   dataset of Fletcher and Thomas (2007b) using *PCOrd v.6.08* (McCune & Mefford 1999).

275   We reclassified the alpine vegetation type in Fletcher and Thomas (2007b) to montane

276   rainforest and alpine (treeless) vegetation based on the vegetation data presented in that

277   paper, and we performed the same data pre-treatment used in Fletcher and Thomas (2007b):

278   using a reduced 32 taxa pollen dataset and recalculating the relative values from this

279   reduced sum. Changes in palynological richness and the rate-of-change (RoC) were

280   computed using *Psimpol* (Bennett, 1994). The data were interpolated to 75-year time-steps

281   (the median sample resolution for the record) to meet the requirements of the RoC analysis

282   and the squared chord distance metric was selected as the distance measure.

283

284   Granger Causality tests (Granger, 2001) were performed to quantitatively test the lagged

285   association between *Eucalyptus* abundance and fire (CHAR). This statistical analysis is

286   based on two principles: 1) a "cause" happens prior to its "effect" and 2) a "cause" has

287   unique information about the future values of its "effect" (Granger 1980). In other words,

288   the Granger Causality test is a statistical hypothesis test for determining whether one time

289   series is useful in forecasting another (Granger 1980). We ran two sets of Granger Causality

290   Tests using *Eucalyptus* percent data and CHAR from the late Pleistocene (18-11.7 kcal BP)

291   and Holocene (11.7-0 kcal BP). Each set is characterised by two hypotheses: "*Eucalyptus*

292   leads charcoal" and "Charcoal leads *Eucalyptus:* if the 95% significance level is reached

293   (p-value <0.05), the hypothesis is accepted. The time series were tested for stationarity,

294   differenced to remove trends and interpolated to equal time windows (75-year bins) prior

295   to analysis. Tests were performed up to 8 lag steps (560 years). Granger Causality was

296   considered superior to another commonly used temporal correlation test, Superposed

297   Epoch Analysis (SEA) (used in Fletcher et al, 2020), due to the absence of obvious "events"

298   in our timeseries data that are required for *a priori* input for SEA. Rather, Granger Causality

299   allows a test of the overall temporal relationship between two timeseries, not just the

300   relationship between selected events in one series against trends in a secondary series.

301   Dating of TAS1508N1 revealed ca. 9 kcal BP of sediment accumulation that allowed an

302   assessment of the comparability of the pollen stratigraphy from the shallower and deeper

303   coring locations (Fig. 2).

304

305   **4. Results**

306   *4.1 Chronology*

307   The results of the ^{210}Pb and radiocarbon analyses are presented in Tables 1 and 2, along

308   with their calibrated radiocarbon age and age uncertainty. Unsupported ^{210}Pb activity

309   reached background at 5 cm (Beck et al. 2019). We selected the Constant Initial

310   Concentration (CIC) modelled ^{210}Pb ages (Appleby 2001) as the deep anoxic conditions at

311   Lake Vera (see Beck et al. 2018) imply that sedimentation rates would be relatively linear.

312   No age reversals were evident in the age-model determinations for the cores used in the

313   composite sequence (TAS1108SC1 and TAS1108LCA). The *Clam* age-depth modelling

314   for the composite core produced a relatively linear model with slower accumulation rates

315   prior to *ca.*16 kcal BP than in the rest of the sequence (Fig. 2).

316

317   *4.2 Charcoal analysis and core correlation*

318   The composite and adjusted CHAR record is displayed in Fig. 3a. The overlap in

319   independently dated CHAR stratigraphies identified a clear splice-point between

320   TAS1108SC and TAS1108LCA at 91-cm in TAS1108SC (28-cm in TAS1108LCA) –

321   *ca.*2.3 kcal BP (Fig. S2; Appendix S2). The period between *ca.*18-16.2 kcal BP was

322   characterised by low, increasing CHAR values**.** A sharp rise in CHAR occurred at *ca.*16.2

323   kcal BP and high values lasted until *ca.*15 kcal BP, followed by lower (on average), but

324   variable values until *ca.*13.5 kcal BP. Peak CHAR values for the early part of the record

325   occurred at *ca.*13 kcal BP, and CHAR remained relatively high until *ca.*12 kcal BP. The

326   period between *ca.*12-2.4 kcal BP was marked by low CHAR values, after which three

327   CHAR peaks occurred at 2.4 kcal BP, 1.3 kcal BP, and 0.6 kcal BP. The period between

328   *ca.*1.5-0.6 kcal BP was characterised by elevated CHAR values.

329

330   The regime-shift analysis identified eight CHAR zones (Fig. 3, Fig. S2; Appendix S2): a

331   low CHAR phase between *ca.*18-16 kcal BP; high CHAR between *ca.*16-15 kcal BP; lower

332   CHAR between *ca.*15-13 kcal BP (but remains high relative to the overall record); high

333　CHAR between *ca.*13-12 kcal BP; very low CHAR between *ca.*12-2.4 kcal BP; high

334　CHAR between *ca.*2.4-1.5 kcal BP; a further shift toward high values between *ca.*1.5-0.6

335　kcal BP; and a drop in CHAR between *ca.*0.6 kcal BP and the present.

336

337　*4.3 Palynology*

338　Six key pollen zones were identified with the aid of CONISS, with each zone split into

339　subzones for ease of description (Fig. 4). Descriptions of each pollen zone are provided in

340　Table 3.

341

342　*4.4 Data analysis*

343　DCA Axis 1 explained 61.7% of the variance in long-term vegetation change (Fig. 3d),

344　according to the ordination analysis performed on the fossil pollen data alone. A major

345　shift in species composition (manifest principally as a switch from *Lagarostrobos*

346　dominance to *Eucryphia* dominance) occurred at *ca.*2.4 kcal BP immediately following a

347　CHAR peak (Fig. 3a, d). The period from *ca.*2.4 kcal BP to present featured high frequency

348　compositional shifts in response to fluctuating CHAR values. The second DCA analysis

349　performed on the fossil pollen dataset from Lake Vera combined with the modern pollen

350　dataset of Fletcher and Thomas (2007b) reveals clear compositional shifts through time

351　(Fig. 5). The initial pollen zone (LV zone 1) was a 'non-analogue' assemblage (i.e. did not

352　overlap with any modern pollen assemblage in the DCA ordination space) driven by high

353　Poaceae values. This zone indicates the presence of a late-Pleistocene grass-dominant

354　landscape, which is also registered at other sites in Tasmania at this time (Colhoun 2000).

355　The next two pollen zones (LV zones 2 and 3) overlap with samples from present-day

356 montane rainforest, reflecting the establishment of this vegetation type as temperature

357 increased through the LGIT. Zones 4-6 overlap with modern lowland rainforest samples,

358 marking the development of the present-day rainforest vegetation.

359

360 The rarefaction analysis shows an increase in pollen richness at *ca.*16 kcal BP: variable but

361 overall relatively high floristic richness until *ca.*13.5 kcal BP; a decrease in richness

362 between *ca.*13.5-7 kcal BP; lowest richness between *ca.*7-2.4 kcal BP; and an increase from

363 *ca.*2.4 kcal BP to the present (Fig. 3c). The RoC analysis indicates overall low rates of

364 change between *ca.*18-2.4 kcal BP, with slightly elevated values between *ca.*15-8 kcal BP

365 (Fig. 3e). A sharp rise in the RoC occurred at *ca.*2.4 kcal BP and again at *ca.*0.6 kcal BP.

366

367 P-values derived for the quantitative Granger Causality test (i.e. temporal association

368 between *Eucalyptus* percent abundance and fire) are displayed in Fig. 6. Low p-values

369 (<0.05) for "Charcoal leads *Eucalyptus*" in the late Pleistocene and "*Eucalyptus* leads

370 charcoal" in the Holocene allow a tentative acceptance of these hypotheses. Significance

371 levels were reached for all lags in these two panels, revealing an immediate (within 75-

372 year) and long-term (up to 560-years) significant relationship. Inspection of *Eucalyptus*

373 pollen against charcoal signals for these time periods (Fig. S3; Appendix S3) supports these

374 tentative hypotheses, showing that prior to the Holocene, increases in *Eucalyptus* followed

375 increases in charcoal, while the reverse response (i.e. *Eucalyptus* expansion preceded

376 periods of increased fire activity) prevailed during the most recent ~12 ka.

377

378 **5. Discussion**

379   *5.1 Long-term climatic change and rainforest vegetation dynamics*

380   Our results indicate replacement of grassland by montane rainforest taxa (Cupressaceae

381   and *N. gunnii*) at *ca.*17.8 kcal BP, synchronous with warming in Antarctica (Fig. 7) and

382   with the expansion of rainforest taxa across the southern mid-latitudes (Vandergoes et al.

383   2013; Moreno et al. 2015). These trends indicate a tight coupling between high- and mid-

384   latitude temperature change and vegetation dynamics across the Southern Hemisphere at

385   that time. Despite evidence for increased fire activity within the local catchment, rainforest

386   expanded through the late Pleistocene at Lake Vera (Figs. 3,4,7). The high pollen

387   taxonomic richness during this phase (*ca.*16-12 kcal BP) (Fig. 3c) likely reflects a period

388   of re-assortment of vegetation within the pollen catchment in response to both rapid

389   climatic change and increasing fire (Fig. 7). Importantly, the significant Granger Causality

390   result for 'Charcoal leads *Eucalyptus*' at this time (Fig. 6) suggests that climate-driven fires

391   drove an increase in *Eucalyptus* species, consistent with the ecology of cold climate

392   *Eucalyptus* species in the region (*E. vernicosa* and *E. coccifera*), which, while tolerant and

393   favoured by fire, do not require fire for reproduction or recruitment (Kirkpatrick &

394   Harwood 1980). The increase in the cool-climate rainforest pioneer tree, *P. aspleniifolius*,

395   which readily colonises burned ground adjacent to rainforest (Hill & Read 1984), also

396   likely reflects the influence of fire within the local catchment. The period between *ca.* 18-

397   12 kcal BP is a phase during which the principal source of rainfall for the region, southern

398   westerly winds, contracted southward and away from Tasmania (Anderson et al. 2009;

399   Denton et al. 2010), thus, increasing the probability of fire in this landscape (Mariani &

400   Fletcher 2016; Mariani & Fletcher 2017). We also observe a continuation of the tight

401   hemispheric coupling of climate and vegetation dynamics through the millennial-scale

402   climate event known as the Antarctic Cold Reversal (ca.14.7-13 kcal BP; Pedro et al. 2016),

403   with a clear reduction in charcoal and pollen from rainforest trees at Lake Vera (Figs 3,4,7)

404   that is consistent with a shift to cooler and wetter conditions reported across rainforest

405   dominant parts of the southern mid-latitudes (Moreno 2004; Vandergoes et al. 2008;

406   Putnam et al. 2010; Pedro et al. 2016).

407

408   The establishment of an essentially modern lowland rainforest around Lake Vera occurred

409   by *ca.*12 kcal BP (pollen zone LV5) (Fig. 4) and is associated with a sharp decrease in

410   CHAR values through the subsequent *ca.* 9 kcal yrs (*ca.*12-2.4 kcal BP; Figs. 3,4,7). This

411   low fire period at Lake Vera stands in stark contrast to the highly variable trends in fire

412   activity between *ca.* 12-3 kcal BP recorded immediately upslope from Lake Vera (Figs

413   1,7f) (Fletcher et al. 2015) and across western Tasmania (Rees et al. 2015; Mariani &

414   Fletcher 2017; Stahle et al. 2017). Indeed, the period between ca. 12-8 kcal BP is

415   recognised as a period of drying across a broad swath of the southern mid-latitudes

416   resulting from an attenuation of westerly circulation (Fletcher & Moreno 2012) that, in

417   combination with peak Holocene temperatures (Shakun & Carlson 2010), resulted in

418   increased biomass burning and low lake levels in many mid-latitude southern hemisphere

419   locations (Moreno et al. 2010; Fletcher & Moreno 2012; Wilkins et al. 2013; Pesce &

420   Moreno 2014; Fletcher et al. 2015; Rees et al. 2015; Mariani & Fletcher 2017).

421   Interestingly, while the vegetation at Lake Vera during this phase (pollen zone LV3) was

422   dominated by a fire-sensitive montane rainforest assemblage (Fig. 7), there is a marked

423   increase in fern spores between *ca.*12-8 kcal BP (Fig. 7e). One possible explanation for

424   this trend is via the role of moisture stress in causing stress in trees, thinning and opening

425   the forest canopy (Hartshorn 1978), thus, increasing light penetration to the forest floor that

426   favours light-demanding species, such as ferns (Nakagawa et al. 2000).

427

428   The substantial reduction in *P. aspleniifolius* and concomitant increase in *Atherosperma*

429   *moschatum* and *N. cunninghamii* at *ca.*12 kcal BP can be inferred as a response to both the

430   decrease in moisture and increase in temperature at this time. Both *A. moschatum* and *N.*

431   *cunninghamii* are temperate rainforest taxa tolerant of drier and warmer conditions relative

432   to *P. aspleniifolius* (Read & Busby 1990), and these trends reflect the establishment of a

433   warmer and drier rainforest assemblage, synchronous with similar compositional changes

434   in Chilean rainforests through this phase of peak Holocene temperature (Shakun & Carlson

435   2010) and southern mid-latitude drying (Fig. 7g) (Moreno 2004; Pesce & Moreno 2014).

436   Further evidence of climate-driven rainforest dynamics in the absence of fire is evident in

437   the substantial increase in the hyper-fire sensitive conifer, *Lagarostrobos franklinii*, at Lake

438   Vera at *ca.*5 kcal BP. *L. franklinii* is a mast seeding species for which dry spring-summers

439   initiate floral ignition and seed production (Fletcher 2015). This trend is mirrored across

440   many sites in western Tasmania (Fletcher 2015) and is concomitant with a raft of evidence

441   that suggests a shift toward higher-frequency moisture variability in southeast Australia

442   after *ca.*5 kcal BP (Donders et al. 2007) following the intensification of the ENSO climate

443   system (Figs 6 h,i) (Moy et al. 2002).

444

445   Following the *ca.* 9 kcal BP of very low fire activity and substantial re-assortment of

446   rainforest composition in response to climatic change at Lake Vera between *ca.* 12-2.4 kcal

447   BP, a large local fire event at *ca.*2.4 kcal BP occurred. This fire 'event' was composed of

448 one or more closely spaced events, in concert with a sharp spike in fire activity immediately

449 upslope (Fletcher et al. 2015) (Figs 6a,f) and across much of western Tasmania (Fletcher

450 et al. 2014; Rees et al. 2015; Stahle et al. 2016; Mariani & Fletcher 2017). This regional

451 peak in fire activity occurred during a millennial-scale phase of high frequency El Niño

452 events recorded in the tropical east Pacific (Fig. 7i) (Moy et al. 2002; Conroy et al. 2008)

453 and a period of pronounced moisture deficit and a concomitant step-wise increase in fire

454 activity in western Tasmania (Fletcher et al. 2015; Mariani & Fletcher 2017). At Lake Vera,

455 the pollen record indicates that this fire event drove a substantial decrease in pollen from

456 *L. franklinii*, consistent with the pyrophobic nature of this rainforest conifer (Hill &

457 Brodribb 1999), along with increases in the rate of change (Fig. 3e) and of forest taxa fond

458 of disturbance, such as *Eucalyptus*, *Eucryphia*, Urticaceae, *Bauera rubioides* and ferns

459 (Fig. 4).

460

461 *5.2 Fire and* Eucalyptus *invasion*

462 While the initial climate-driven Holocene fire event at *ca.*2.4 kcal BP at Lake Vera

463 precedes the increase in *Eucalyptus* pollen at that site, the significant Granger Causality

464 result for '*Eucalyptus* leads charcoal' in the Holocene (Fig. 6) suggests that under a

465 Holocene climate regime, while fire is required to initially facilitate the establishment of

466 lowland *Eucalyptus* species within rainforest vegetation, once this 'fire-weed' is

467 established, the highly flammable foliage of *Eucalyptus* acts as a positive feedback switch

468 (Wilson & Agnew 1992) that promotes further fire, favouring the further recruitment of

469 *Eucalyptus* (Fletcher et al. 2020). Indeed, over the most recent *ca*. 2.4 kcal at Lake Vera,

470 fires occur under anomalously dry climate conditions (Fletcher et al. 2018a), consistent

471   with the requirement for anomalously low rainfall for fires to burn modern Tasmanian

472   rainforests (Styger & Kirkpatrick 2015). The lead of *Eucalyptus* over charcoal reported in

473   the Granger Causality test indicates that the presence of *Eucalyptus* 'guarantees' burning

474   of rainforest under the right set of climatic conditions. This stands in stark contrast with

475   the lack of early Holocene (*ca*. 12-8 kcal BP) charcoal signature at Lake Vera while

476   Eucalypt values were low, despite evidence for regional drying and increased fire activity

477   (Fletcher & Thomas 2010; Rees et al. 2015; Stahle et al. 2016; Mariani & Fletcher 2017;

478   Stahle et al. 2017) – a finding that is consistent with the requirement of *Eucalyptus*

479   occurrence to trigger a shift from pyrophobic rainforest at pyrophytic vegetation in

480   montane rainforests in Tasmania (Fletcher et al. 2020).

481

482   The prolonged period of low to absent fire activity at Lake Vera between *ca*. 12-2.4 kcal

483   BP (indicating either reduced frequency and/or severity of burning) is concomitant with a

484   drop in *Eucalyptus* values that indicates a decline within the local vegetation (Figs. 3,4)

485   (Fletcher & Thomas 2007b). In contrast, sites that record increasing charcoal during the

486   hemisphere-wide drying phase in the early-Holocene (*ca*. 12-8 kcal BP) were instead

487   dominated by more open fire-promoted plant communities (Macphail 1979; Fletcher &

488   Thomas 2007b; Rees et al. 2015; Stahle et al. 2016; Stahle et al. 2017). We contend that

489   the onset of an interglacial (Holocene) climate regime at *ca*. 12 kcal BP facilitated the

490   capturing of the local Lake Vera catchment by low-flammability rainforest species that

491   effectively negated fire (sensu Wood & Bowman 2012) and maintained relative stability in

492   the vegetation landscape (i.e. low RoC values (Fig. 3e)) at a time when regional fire activity

493   was increasing (Fletcher & Thomas 2007a; Fletcher & Thomas 2010; Rees et al. 2015;

494   Stahle et al. 2016; Mariani & Fletcher 2017; Stahle et al. 2017). A combination of low

495   rainforest fuel flammability (Wood & Bowman 2012) and topographic setting (a steep and

496   predominantly south-facing aspect) (Wood et al. 2011) likely permitted the establishment

497   of fire-resistant rainforest within the Lake Vera catchment, while more exposed

498   topographic sites experienced burning in response to regional hydroclimatic change

499   (Fletcher & Thomas 2010).

500

501   The contrast in *Eucalyptus*-fire dynamics between the late Pleistocene and Holocene

502   identified by the Granger Causality tests (Fig. 6) may be explained by the diversity of fire

503   ecologies evident within the *Eucalyptus* genus. While the cool climate *Eucalyptus* species

504   in the region today do not require fire for reproduction (Kirkpatrick & Harwood 1980),

505   lowland wet forest *Eucalyptus* species, such as *E. regnans*, *E. nitida* and *E. ovata* (also

506   present within the region today) require fire for regeneration, and these species actively

507   promote fire via the production and accumulation of abundant highly flammable fuels

508   (Ashton 1981). Spatially, it is likely that the late-Holocene increase in *Eucalyptus* in the

509   Lake Vera pollen record (Fig. 3f) marks the establishment of *Eucalyptus* forest on the

510   relatively drier NW (windward) facing slope of the catchment (see Fig. 1). Importantly, for

511   the long-term persistence of this rainforest, it is unclear whether a threshold of flammable

512   species content within the catchment has been crossed in this system and a transition of the

513   catchment to a Eucalypt-forest is inevitable (Beck et al. 2018). This is particularly

514   concerning, given (1) the clear increase in regional fire activity over the last 500 years in

515   Tasmania, resulting from both 'natural' and anthropogenic climate trends (Mariani &

516   Fletcher 2016), (2) the projected increase in fire activity in temperate regions in response

517   to climate change (Moritz et al. 2012) and (3) the increasing human activity in this popular

518   tourist destination.

519

520   **Conclusions**

521   We record a shift from a grass-dominant landscape in the late Pleistocene to rainforest-

522   dominance in this steep-sided and topographically sheltered catchment in southwest

523   Tasmania during the Last Glacial-Interglacial Transition, a time when flammable

524   vegetation became the dominant regional vegetation type in response to cultural burning

525   by the Indigenous Palawa people of Tasmania. We demonstrate a highly responsive cool

526   temperate rainforest system to climatic change in the absence of local-scale fire in a

527   landscape dominated by flammable vegetation types. Indeed, the negative feedback

528   between rainforest vegetation and fire (via low fuel flammability) resulted in a prolonged

529   (9 kcal yr) phase of low to absent fire activity through the early and mid-Holocene despite

530   proximal sites recording large increases in early-Holocene fire activity. Establishment of

531   Eucalypts following fire in the late-Holocene has altered the vegetation-fire dynamic,

532   dramatically increasing the probability of burning of the local catchment vegetation and

533   heralding a significant threat to the long-term security of this endangered vegetation type.

534

535   **Acknowledgements**

545

546 Data Availability

547 Data   a   freely   available   via   contacting   Michael-Shawn   Fletcher

548 (michael.fletcher@unimelb.edu.au) and will be placed on NEOTOMA upon acceptance

549 for publication (https://www.neotomadb.org/).

550
551

552 **6.** References
553
554 Anderson, R.F., Ali, S., Bratmiller, L.I., Nielsen, S.H.H., Fleisher, M.Q., Anderson, B.E.

555 & Burkle, L.H. 2009. Wind-Driven Upwelling in the Southern Ocean and the Deglacial

556 Rise in Atmospheric CO_2. *Science* 323: 1443-1448.

557 Appleby, P. 2001. Chronostratigraphic techniques in recent sediments. In: Last, W.M. &

558 Smol, J.P. (eds.) *Tracking Environmental Change Using Lake Sediments*, pp. 171-203.

559 Kluwer Academic Publishers, Dordrecht, THe Netherlands.

560 Ashton, D. 1981. The ecology of the boundary between Eucalyptus regnans F. Muell. and

561 E. obliqua L'Herit. *Victoria. Proceedings of the Ecological Society of Australia* 11: 75-

562 94.

563 Beck, K.K., Fletcher, M.-S., Gadd, P.S., Heijnis, H. & Jacobsen, G.E. 2017. An early

564 onset of ENSO influence in the extra-tropics of the southwest Pacific inferred from a 14,

565 600 year high resolution multi-proxy record from Paddy's Lake, northwest Tasmania.

566 *Quaternary Science Reviews* 157: 164-175.

567 Beck, K.K., Fletcher, M.S., Gadd, P.S., Heijnis, H., Saunders, K.M., Simpson, G.L. &

568 Zawadzki, A. 2018. Variance and rate‐of‐change as early warning signals for a critical

569 transition in an aquatic ecosystem state: a test case from Tasmania, Australia. *Journal of*

570 *Geophysical Research: Biogeosciences* 123: 495-508.

571 Blaauw, M. 2010. Methods and code for 'classical'age-modelling of radiocarbon

572 sequences. *Quaternary Geochronology* 5: 512-518.

573   Bond, W.J. & Midgley, J.J. 1995. Kill thy neighbour: an individualistic argument for the

574   evolution of flammability. *Oikos*: 79-85.

575   Bowman, D. 2000. *Australia rainforests: islands of green in an ocean of fire*. Cambridge

576   University Press, Cambridge.

577   Bowman, D.M., Murphy, B.P., Neyland, D.L., Williamson, G.J. & Prior, L.D. 2014.

578   Abrupt fire regime change may cause landscape‐wide loss of mature obligate seeder

579   forests. *Global change biology* 20: 1008-1015.

580   Brooks, M.L., D'Antonio, C.M., Richardson, D.M., Grace, J.B., Keeley, J.E., DiTomaso,

581   J.M., Hobbs, R.J., Pellant, M. & Pyke, D. 2004. Effects of invasive alien plants on fire

582   regimes. *BioScience* 54: 677-688.

583   Cadd, H., Fletcher, M.-S., Mariani, M., Heijnis, H. & Gadd, P.S. 2019. The influence of

584   fine‐scale topography on the impacts of Holocene fire in a Tasmanian montane

585   landscape. *Journal of Quaternary Science* 34: 491-498.

586   Colhoun, E.A. 2000. Vegetation and climate during the last interglacial–glacial cycle in

587   western Tasmania, Australia. *Palaeogeography, Palaeoclimatology, Palaeoecology* 155:

588   195-209.

589   Conroy, J.L., Overpeck, J.T., Cole, J.E., Shanahan, T.M. & Steinitz-Kannan, M. 2008.

590   Holocene changes in eastern tropical Pacific climate inferred from a Galápagos lake

591   sediment record. *Quaternary Science Reviews* 27: 1166-1180.

592   Cosgrove, R. 1999. Forty-two degrees south: the archaeology of Late Pleistocene

593   Tasmania. *Journal of World Prehistory* 13: 357-402.

594   Cullen, P. 1991. Regeneration of *Athrotaxis selaginoides* and other rainforest tree species

595   on landslide faces in Tasmania. In: al., M.B.e. (ed.) *Aspects of Tasmanian Botany - a*

596   *tribute to Winifred Curtis*. Royal Society of Tasmania, Hobart.

597   Cullen, P.J. 1987. Regeneration patterns in populations on *Athrotaxis selaginoides* D.

598   Don. from Tasmania. *Journal of Biogeography* 14: 39 - 51.

599   Cullen, P.J. & Kirkpatrick, J.A. 1988a. The Ecology of *Athrotaxis* D. Don (Taxodiaceae).

600   II. The Distributions and Ecological Differentiation of *A. cupressoides* and *A.*

601   *selaginoides*. *Australian Journal of Botany* 36: 561 - 573.

602   Cullen, P.J. & Kirkpatrick, J.A. 1988b. The Ecology of *Athrotaxis* D. Don.

603   (Taxodiaceae). I. Stand Structure and Regeneration of *A. cupressoides*. *Australian*

604   *Journal of Botany* 36: 547 - 560.

605   Denton, G.H., Anderson, R.F., Toggweiler, J.R., Edwards, R.L., Schaefer, J.M. &

606   Putnam, A.E. 2010. The Last Glacial Termination. *Science* 328: 1652.

607   Donders, T.H., Haberle, S., Hope, G., Wagner, F. & Visscher, H. 2007. Pollen evidence

608   for the transition of the Eastern Australian climate system from the post-glacial to the

609   present-day ENSO mode. *Quaternary Science Reviews* 26: 1621-1637.

610   Enright, N.J., Fontaine, J.B., Bowman, D.M., Bradstock, R.A. & Williams, R.J. 2015.

611   Interval squeeze: altered fire regimes and demographic responses interact to threaten

612   woody species persistence as climate changes. *Frontiers in Ecology and the Environment*

613   13: 265-272.

614   Faegri, K. & Iversen, J. 1989. *Textbook of pollen analysis*. Wiley, New York.

615   Fletcher, M.-S. 2015. Mast seeding and the El Niño-Southern Oscillation: a long-term

616   relationship? *Plant Ecology*: 1-7.

617   Fletcher, M.-S., Benson, A., Bowman, D.M., Gadd, P.S., Heijnis, H., Mariani, M.,

618   Saunders, K.M., Wolfe, B.B. & Zawadzki, A. 2018a. Centennial-scale trends in the

619   Southern Annular Mode revealed by hemisphere-wide fire and hydroclimatic trends over

620   the past 2400 years. *Geology* 46: 363-366.

621   Fletcher, M.-S., Benson, A., Heijnis, H., Gadd, P.S., Cwynar, L.C. & Rees, A.B.H. 2015.

622   Changes in biomass burning mark the onset an ENSO-influenced climate regime at 42°S

623   in southwest Tasmania, Australia. *Quaternary Science Reviews* 122: 222-232.

624   Fletcher, M.-S., Bowman, D., Whitlock, C., Mariani, M. & Stahle, L. 2018b. The

625   changing role of fire in conifer-dominated temperate rainforest through the last 14,000

626   years. *Quaternary Science Reviews* 182: 37-47.

627   Fletcher, M.-S., Cadd, H., Mariani, M., Hall, T. & Wood, S.W. 2020. The role of species

628   composition in the emergence of alternate vegetation states in a temperate rainforest

629   system. *Landscape Ecology*.

630   Fletcher, M.-S. & Moreno, P.I. 2012. Have the Southern Westerlies changed in a zonally

631   symmetric manner over the last 14,000 years? A hemisphere-wide take on a controversial

632   problem. *Quaternary International* 253: 32–46.

633   Fletcher, M.-S. & Thomas, I. 2007a. Holocene vegetation and climate change from near

634   Lake Pedder, south-west Tasmania, Australia. *Journal of Biogeography* 34: 665-677.

635   Fletcher, M.-S. & Thomas, I. 2007b. Modern pollen–vegetation relationships in western

636   Tasmania, Australia. *Review of Palaeobotany and Palynology* 146: 146-168.

637   Fletcher, M.-S. & Thomas, I. 2010. The origin and temporal development of an ancient

638   cultural landscape. *Journal of Biogeography* 37: 2183–2196.

639   Fletcher, M.-S., Wolfe, B.B., Whitlock, C., Pompeani, D.P., Heijnis, H., Haberle, S.G.,

640   Gadd, P.S. & Bowman, D.M.J.S. 2014. The legacy of mid-Holocene fire on a Tasmanian

641   montane landscape. *Journal of Biogeography* 41: 476-488.

642   Granger, C.W. 1980. Testing for causality: a personal viewpoint. *Journal of Economic*

643   *Dynamics and control* 2: 329-352.

644   Grimm, E. 1987. CONISS: A FORTRAN 77 program for stratigraphically constrained

645   cluster analysis by the method of incremental sum of squares. *Computers & Geosciences*

646   13: 13-35.

647   Harris, R.M.B., Beaumont, L.J., Vance, T.R., Tozer, C.R., Remenyi, T.A., Perkins-

648   Kirkpatrick, S.E., Mitchell, P.J., Nicotra, A.B., McGregor, S., Andrew, N.R., Letnic, M.,

649   Kearney, M.R., Wernberg, T., Hutley, L.B., Chambers, L.E., Fletcher, M.S., Keatley,

650 M.R., Woodward, C.A., Williamson, G., Duke, N.C. & Bowman, D.M.J.S. 2018.

651 Biological responses to the press and pulse of climate trends and extreme events. *Nature*

652 *Climate Change* 8: 579-587.

653 Harris, S. & Kitchener, A. 2005. From forest to fjaeldmark: Descriptions of Tasmania's

654 vegetation. In: Department of Primary Industries, W.a.E. (ed.), Hobart, Tasmania.

655 Hartshorn, G. 1978. *Tree falls and tropical forest dynamics*. Cambridge University Press,

656 New York.

657 Hill, R.S. & Brodribb, T.J. 1999. Southern Conifers in Time and Space. *Australian*

658 *Journal of Botany* 47: 639-969.

659 Hill, R.S. & Read, J. 1984. Post-fire regeneration of rainforest and mixed forest in

660 western Tasmania. *Australian Journal of Botany* 32: 481-493.

661 Hogg, A.G., Heaton, T.J., Hua, Q., Palmer, J.G., Turney, C.S., Southon, J., Bayliss, A.,

662 Blackwell, P.G., Boswijk, G. & Ramsey, C.B. 2020. SHCal20 Southern Hemisphere

663 calibration, 0–55,000 years cal BP. *Radiocarbon*: 1-20.

664 Hogg, A.G., Hua, Q., Blackwell, P.G., Niu, M., Buck, C.E., Guilderson, T.P., Heaton,

665 T.J., Palmer, J.G., Reimer, P.J. & Reimer, R.W. 2013. SHCal13 Southern Hemisphere

666 calibration, 0–50,000 cal yr BP. *Radiocarbon*.

667 Holz, A., Wood, S.W., Veblen, T.T. & Bowman, D.M. 2015. Effects of high severity fire

668 drove the population collapse of the subalpine Tasmanian endemic conifer Athrotaxis

669 cupressoides. *Global change biology*.

670 Holz, A., Wood, S.W., Ward, C., Veblen, T.T. & Bowman, D.M. 2020. Population

671 collapse and retreat to fire refugia of the Tasmanian endemic conifer Athrotaxis

672 selaginoides following the transition from Aboriginal to European fire management.

673 *Global change biology* 26: 3108-3121.

674 Jackson, W.D. 1968. Fire, air, water and earth - An elemental ecology of Tasmania.

675 *Proceedings of the Ecological Society of Australia* 3: 9-16.

676 Jackson, W.D. 1999. The Tasmanian environment. In: Reid, J.B., Hill, R.S., Brown, M.J.

677 & Hovenden, M.J. (eds.) *Vegetation of Tasmania*. Australian Biological Resources Study,

678 Canberra.

679 Juggins, S. 2012. Package 'rioja': Analysis of Quaternary Science Data. In. University of

680 Newcastle, Newcastle-upon-Tyne.

681 Kirkpatrick, J. & Dickinson, K. 1984. The impact of fire on Tasmanian alpine vegetation

682 and soils. *Australian Journal of Botany* 32: 613-629.

683 Kirkpatrick, J.B. & Harwood, C.E. 1980. The vegetation of an infrequently burned

684 Tasmanian mountain region. *Proceedings of the Royal Society of Victoria* 91: 79-107.

685 Macphail, M.K. 1979. Vegetation and climates in southern Tasmania since the last

686 glaciation. *Quaternary Research* 11: 306-341.

687 Mariani, M., Connor, S.E., Fletcher, M.S., Theuerkauf, M., Kuneš, P., Jacobsen, G.,

688 Saunders, K.M. & Zawadzki, A. 2017. How old is the Tasmanian cultural landscape? A

689   test of landscape openness using quantitative land ‐ cover reconstructions. *Journal of*

690   *Biogeography*.

691   Mariani, M. & Fletcher, M.-S. 2017. Long-term climate dynamics in the extra-tropics of

692   the South Pacific revealed from sedimentary charcoal analysis. *Quaternary Science*

693   *Reviews* 173: 181-192.

694   Mariani, M. & Fletcher, M.S. 2016. The Southern Annular Mode determines inter ‐

695   annual and centennial ‐ scale fire activity in temperate southwest Tasmania, Australia.

696   *Geophysical Research Letters* 43.

697   Mariani, M., Fletcher, M.S., Haberle, S., Chin, H., Zawadzki, A. & Jacobsen, G. 2019.

698   Climate change reduces resilience to fire in subalpine rainforests. *Global change biology*

699   25: 2030-2042.

700   Marsden-Smedley, J.B. 1998. Changes in southwestern Tasmanian fire regimes since the

701   early 1800's. *Papers and Proceedings of the Royal Society of Tasmania* 132: 15-29.

702   McCune, B. & Mefford, M.J. 1999. PC-Ord for Windows. In. MjM Software, Gleneden

703   Beach, OR.

704   McKemey, M., Costello, O., Ridges, M., Ens, E.J., Hunter, J.T. & Reid, N.C. 2020. A

705   review of contemporary Indigenous cultural fire management literature in southeast

706   Australia.

707   Moreno, P.I. 2004. Millennial-scale climate variability in northwest Patagonia over the

708   last 15000 yr. *Journal of Quaternary Science* 19: 35-47.

709   Moreno, P.I., Denton, G.H., Moreno, H., Lowell, T.V., Putnam, A.E. & Kaplan, M.R.

710   2015. Radiocarbon chronology of the last glacial maximum and its termination in

711   northwestern Patagonia. *Quaternary Science Reviews* 122: 233-249.

712   Moreno, P.I., Francois, J.P., Moy, C.M. & Villa-Martinez, R. 2010. Covariability of the

713   Southern Westerlies and atmospheric CO2 during the Holocene. *Geology* 38: 727-730.

714   Moritz, M.A., Parisien, M.-A., Batllori, E., Krawchuk, M.A., Van Dorn, J., Ganz, D.J. &

715   Hayhoe, K. 2012. Climate change and disruptions to global fire activity. *Ecosphere* 3:

716   art49.

717   Morris, J.L., Brunelle, A., DeRose, R.J., Seppä, H., Power, M.J., Carter, V. & Bares, R.

718   2013. Using fire regimes to delineate zones in a high-resolution lake sediment record

719   from the western United States. *Quaternary Research* 79: 24-36.

720   Moy, C.M., Seltzer, G.O., Rodbell, D.T. & Anderson, D.M. 2002. Variability of El

721   Nino/Southern Oscillation activity at millennial timescales during the Holocene. *Nature*

722   420: 162-165.

723   Nakagawa, M., Tanaka, K., Nakashizuka, T., Ohkubo, T., Kato, T., Maeda, T., Sato, K.,

724   Miguchi, H., Nagamasu, H. & Ogino, K. 2000. Impact of severe drought associated with

725   the 1997–1998 El Nino in a tropical forest in Sarawak. *Journal of Tropical Ecology* 16:

726   355-367.

727   Pedro, J.B., Bostock, H.C., Bitz, C.M., He, F., Vandergoes, M.J., Steig, E.J., Chase,

728   B.M., Krause, C.E., Rasmussen, S.O. & Markle, B.R. 2016. The spatial extent and

729   dynamics of the Antarctic Cold Reversal. *Nature Geoscience* 9: 51-55.

730   Pesce, O. & Moreno, P. 2014. Vegetation, fire and climate change in central-east Isla

731   Grande de Chiloé (43 S) since the Last Glacial Maximum, northwestern Patagonia.

732   *Quaternary Science Reviews* 90: 143-157.

733   Putnam, A.E., Denton, G.H., Schaefer, J.M., Barrell, D.J., Andersen, B.G., Finkel, R.C.,

734   Schwartz, R., Doughty, A.M., Kaplan, M.R. & Schlüchter, C. 2010. Glacier advance in

735   southern middle-latitudes during the Antarctic Cold Reversal. *Nature Geoscience* 3: 700-

736   704.

737   Read, J. & Busby, J.R. 1990. Comparative responses to temperature of the major canopy

738   species of Tasmanian cool temperate rainforest and their ecological significance. II. Net

739   photosynthesis and climate analysis. *Australian Journal of Botany* 38: 185-205.

740   Rees, A.B., Cwynar, L.C. & Fletcher, M.-S. 2015. Southern Westerly Winds submit to

741   the ENSO regime: A multiproxy paleohydrology record from Lake Dobson, Tasmania.

742   *Quaternary Science Reviews* 126: 254-263.

743   Rickards, L. 2016. Goodbye Gondwana? Questioning disaster triage and fire resilience in

744   Australia. *Australian Geographer* 47: 127-137.

745   Rodionov, S.N. 2004. A sequential algorithm for testing climate regime shifts.

746   *Geophysical Research Letters* 31: L09204.

747   Schaefer, J.M., Denton, G.H., Barrell, D.J., Ivy-Ochs, S., Kubik, P.W., Andersen, B.G.,

748   Phillips, F.M., Lowell, T.V. & Schlüchter, C. 2006. Near-synchronous interhemispheric

749   termination of the last glacial maximum in mid-latitudes. *Science* 312: 1510-1513.

750   Shakun, J.D. & Carlson, A.E. 2010. A global perspective on Last Glacial maximum to

751   Holocene climate change. *Quaternary Science Reviews*

752   doi:10.1016/j.physletb.2003.10.071.

753   Stahle, L.N., Chin, H., Haberle, S. & Whitlock, C. 2017. Late-glacial and Holocene

754   records of fire and vegetation from Cradle Mountain National Park, Tasmania, Australia.

755   *Quaternary Science Reviews* 177: 57-77.

756   Stahle, L.N., Whitlock, C. & Haberle, S.G. 2016. A 17,000-Year-Long Record of

757   Vegetation and Fire from Cradle Mountain National Park, Tasmania. *Frontiers in*

758   *Ecology and Evolution* 4: 82.

759   Sturman, A.P. & Tapper, N.J. 2006. *The weather and climate of Australia and New*

760   *Zealand*. Oxford University Press, Melbourne.

761   Styger, J. & Kirkpatrick, J.B. 2015. Less than 50 millimetres of rainfall in the previous

762   month predicts fire in Tasmanian rainforest. *Papers and Proceedings of the Royal Society*

763   *of Tasmania* 149: 1-5.

764   Vandergoes, M.J., Dieffenbacher-Krall, A.C., Newnham, R.M., Denton, G.H. & Blaauw,

765   M. 2008. Cooling and changing seasonality in the Southern Alps, New Zealand during

766   the Antarctic Cold Reversal. *Quaternary Science Reviews* 27: 589-601.

767   Vandergoes, M.J., Newnham, R.M., Denton, G.H., Blaauw, M. & Barrell, D.J. 2013. The

768   anatomy of Last Glacial Maximum climate variations in south Westland, New Zealand,

769   derived from pollen records. *Quaternary Science Reviews* 74: 215-229.

770   Whitlock, C. & Larsen, C. 2001. Charcoal as a fire proxy. In: Smol, J.P., Birks, H.J.B. &

771   Last, W.M. (eds.) *Tracking environmental change using lakes sediments*. Kluwer

772   Academic Publishers, Dordrecht, The Netherlands.

773   Wilkins, D., Gouramanis, C., De Deckker, P., Fifield, L.K. & Olley, J. 2013. Holocene

774   lake-level fluctuations in Lakes Keilambete and Gnotuk, southwestern Victoria,

775   Australia. *The Holocene* 23: 784-795.

776   Wilson, J.B. & Agnew, A.D. 1992. Positive-feedback switches in plant communities.

777   *Advances in Ecological Research* 23: 263-336.

778   Wood, S.W. & Bowman, D.M.J.S. 2012. Alternative stable states and the role of fire–

779   vegetation–soil feedbacks in the temperate wilderness of southwest Tasmania. *Landscape*

780   *Ecology*: 1-16.

781   Wood, S.W., Murphy, B.P. & Bowman, D.M. 2011. Firescape ecology: how topography

782   determines the contrasting distribution of fire and rain forest in the south‐west of the

783   Tasmanian Wilderness World Heritage Area. *Journal of Biogeography* 38: 1807-1820.

784

785

786   **Table 1** [210]Pb dating results. CIC = Constant Initial Concentration model.

Core	Original Depth (cm)	Composite depth (cm)	Composite depth midpoint (cm)*	Lab Number	Material Dated	Supported [210]Pb (Bq/kg)	Unsupported [210]Pb (Bq/kg)	CIC Age (cal yr BP)	CIC Age error (yrs)
TAS1108SC1	0-0.5	0-0.5	0.25	OZ-N950	Bulk sediment	31.1 ± 2.5	106 ± 7.0	-54	6.9
TAS1108SC1	0.5-1	0.5-1	0.75	OZ-N951	Bulk sediment	27.6 ± 2.1	64 ± 5.0	-40	7
TAS1108SC1	1.5-2	1.5-2	1.75	OZ-N952	Bulk sediment	27.8 ± 2.1	17.3 ± 2.9	-13	7.7
TAS1108SC1	2.5-3	2.5-3	2.75	OZ-N953	Bulk sediment	24.5 ± 1.9	11.7 ± 2.5	14.5	8.8
TAS1108SC1	5-5.5	5-5.5	5.25	OZ-N954	Bulk sediment	26.2 ± 2.0	1.3 ± 2.4	83	12.5

787

788   **Table 2** Radiocarbon dating results. Calibrations (kcal BP) are based on the Southern Hemisphere calibration curve SHCal20.14C (Hogg et al.

789   2013; Hogg et al. 2020). Suffix numbers associated with TAS1108LCA refer to continuous 1m sections recovered for the core (see Methods).

Core	Original Depth (cm)	Composite depth (cm)	Composite depth midpoint (cm)*	Lab Number	Material Dated	Radiocarbon Age (^{14}C yr BP)	Error (^{14}C yr BP)	δ13C	Age (cal yr BP)**
TAS1108SC1	23-23.5	23-23.5	23.35	OS-92421	Bulk sediment	650	25	-27.72	548-575 (25.6%), 598-649 (69.1%)
TAS1108SC1	50-50.5	50-50.5	50.25	OS-92422	Bulk sediment	1260	30	-27.6	1061-1186 (87.1%), 1216-1261 (7.8%)
TAS1108SC1	81-81.5	81-81.5	81.25	OS-92423	Bulk sediment	2040	30	-27.55	1886-2012 (95%)

TAS1108LCA-1	50-51	87-88	87.5	OS-93613	Bulk sediment	2250	25	-27.51	2153-2318 (95%)
TAS1108LCA-1	74-75	111-112	111.5	OS-93682	Bulk sediment	3260	30	-27.35	3367-3498 (87.2%), 3501-3509 (1.5%), 3531-3556 (6.3%)
TAS1108LCA-1	94-95	131-132	131.5	OS-93683	Bulk sediment	4590	25	-27.58	5053-5189 (58.9%), 5213-5228 (3.2%), 5231-5252 (3.8%), 5257-5316 (29%)
TAS1108LCA-2	159-160	196-197	196.5	OS-93684	Bulk sediment	8090	30	-27.68	8774-8841 (22.6%), 8846-9029 (72.4%)
TAS1108LCA-3	232-233	269-270	269.5	OS-93685	Bulk sediment	11200	35	-27.15	12910-13110 (95%)
TAS1108LCA-3	271-272	308-309	308.5	OS-93614	Bulk sediment	13300	60	-26.84	15726-16149 (95%)
TAS1108LCA-3	281-282	318-319	318.5	OS-93615	Bulk sediment	14900	65	-25.55	17879-18276 (95%)
TAS1108LCA-3	290-291	327-328	327.5	OS-89142	Bulk sediment	15500	70	-20.56	18566-18870 (95%)
TAS1508N1	114-114.5			D-AMS 015676	Plant macrofossil	2060	34	-32.9	1892-2057 (95%)
TAS1508N1	131-131.5			D-AMS 015678	Plant macrofossil	2171	36	-27.7	2009-2181 (79.6%),

								2241-2302 (15.3%)
TAS1508N1	185-185.5		D-AMS 015682	Plant macrofossil	4150	90	-29.2	4422-4839 (95%)
TAS1508N1	195-195.5		D-AMS 017892	Plant macrofossil	3060	28	NA	3078-3094 (3.7%), 3107-3132 (4.2%), 3136-3272 (68.4%), 3285-3341 (18.6%)
TAS1508N1	238-238.5		D-AMS 015680	Plant macrofossil	3875	39	-21	4096-4119 (4.4%), 4145-4408 (90.5%)
TAS1508N1	298-298.5		D-AMS 016846	Plant macrofossil	4501	24	-30.5	4967-5093 (38%), 5096-5144 (10.9%), 5157-5287 (46%)
TAS1508N1	309.5-310		D-AMS 015683	Plant macrofossil	5463	40	-32.5	6024-6047 (2.4%), 6065-6077 (1.2%), 6114-6152 (6.5%), 6175-6303 (84.9%)
TAS1508N1	358.5-359		D-AMS 017893	Plant macrofossil	6703	37	NA	7445-7445 (0.1%), 7460-7598 (94.4%), 7603-7605 (0.4%)

TAS1508N1	359-360		D-AMS 016847	Plant macrofossil	6915	30	-30.8	7624-7647 (4.9%), 7651-7789 (90%)
TAS1508N1	383.5-384		D-AMS 017894	Plant macrofossil	6193	54	NA	6889-7178 (93.1%), 7204-7206 (0.2%), 7216-7238 (1.7%)
TAS1508N1	399-399.5		D-AMS 016852	Plant macrofossil	5884	25	-24.4	6560-6739 (95%)
TAS1508N1	419.5-420		D-AMS 016848	Plant macrofossil	6079	39	-19.4	6753-6764 (1.5%), 6777-6999 (93.5%)
TAS1508N1	448-448.5		D-AMS 016849	Plant macrofossil	6633	28	-29.5	7431-7521 (76.7%), 7533-7564 (18.2%)
TAS1508N1	462-462.5		D-AMS 016850	Plant macrofossil	6955	27	-27.6	7675-7802 (89.9%), 7806-7825 (4.9%)
TAS1508N1	476-476.5		D-AMS 016851	Plant macrofossil	7133	27	-30	7846-7974 (95%)
TAS1508N1	525.5-526		D-AMS 017895	Plant macrofossil	8074	44	NA	8662-8666 (0.3%), 8705-8713 (0.5%), 8716-9030 (94.2%)

790   Tab. 1

791   **Table 3** Table outlining the six CONISS-derived pollen zones for the Lake Vera record.

792   Includes descriptions of pollen taxa assemblages found within each zone. Refer to Fig. 4 for

793   full dataset.

CONISS	Pollen assemblage description
Zone LV1 *ca*. 18.2-13.9 kcal BP	Subzone LV1a (18.7-17 kcal BP): Poaceae, Asteraceae, *Eucalyptus* and Proteaceae dominate.
	Subzone LV1b (17-13.9 kcal BP): Increases in % Cupressaceae and *Nothofagus gunnii* drive an increase in tree pollen abundance. Concomitant decrease in % Poaceae, Asteraceae and *Eucalyptus*. Increases in % Poaceae, Asteraceae and *Eucalyptus,* and decreases in % Cupressaceae and N. *gunnii* evident from 14.7 ka (beginning of ACR).
Zone LV2 *ca*. 13.9-11.7 kcal BP	*Phyllocladus aspleniifolius* and *Eucalyptus* dominate, with the latter decreasing toward the top. There was a notable increase in % *Gymnoschoenus sphaerocephalus*, which is generally underrepresented in pollen records. % *Nothofagus cunninghamii* increases steadily, % *Isoëtes* increases to peak values at *ca.*12.7 kcal BP, before decreasing.
Zone LV3 *ca.* 11.7-8.5 kcal BP	*% P. aspleniifolius* decreases sharply at *ca.*11.7 kcal BP, concomitant with a stepwise increase in *N. cunninghmaii* pollen which dominates the remainder of this zone. % *Eucalyptus* continues to decline, while those of Cupressaceae and Proteaceae (principally *Agastachys odorata*) increases. Values of *Atherosperma moschatum* peak at *ca.*11 kcal BP.
Zone LV4 *ca.* 8.5-5 kcal BP	*% Eucryphia* (likely *Eucryphia lucida*) /*Anodopetalum* increase substantially at *ca.*8.5 kcal BP and again at *ca.*7.4 kcal BP, before peaking at *ca.*6 kcal BP and then decreasing. % *N. cunninghamii* decreases slightly, as does % Cupressaceae and Proteaceae. %*N. gunnii* increase slightly.
Zone LV5 *ca.* 5-2.4 kcal BP	% *Lagarostrobos franklinii* increases steadily, while % *Eucryphia*/*Anodopetalum* and *Isoëtes* decrease.
Zone LV6 *ca.* 2.4 kcal BP to present	Subzone LV6a (2.4-0.6 kcal BP): Dramatic drop in % *L. franklinii* occurs concomitant with a rise in % *Eucryphia*/*Anodopetalum*, Proteaceae, *Bauera rubioides*, Urticaceae and Cyperaceae.

|	Subzone LV6b (0.6 kcal BP - present): % *Bauera rubioides* and *Eucalyptus* increase further. % *P. aspleniifoliu*s recovers slightly after previous declines.

794   Tab. 2.

795
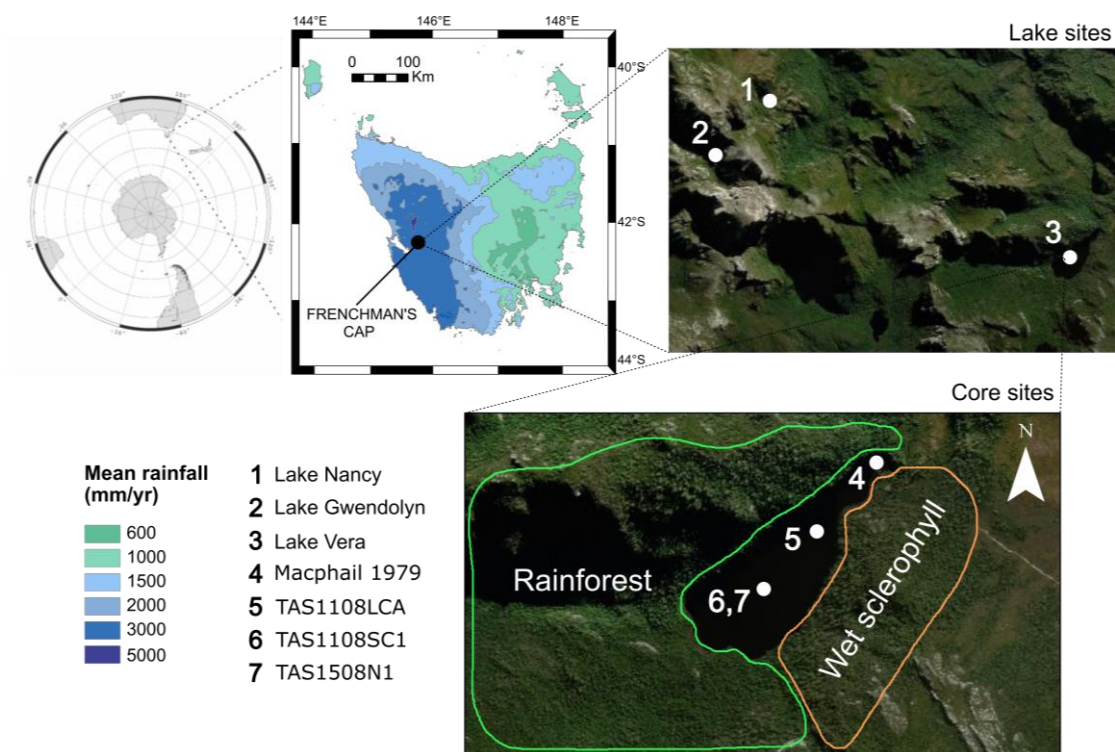
796

797 **Fig. 1** Map of the study area showing the location of Tasmania in the Southern Hemisphere,

798 overlain by average annual rainfall isohyets showing the orographic rainfall gradient across the

799 island, and the location of Lake Vera in relation to other study sites on the Frenchman's Cap,

800 southwest Tasmania, employed by Fletcher et al (2015) (Lake Gwendolyn and Lake Nancy).

801 The lower inset shows the Lake Vera core locations (including an initial core from the site;

802 Macphail 1979) and the distribution of rainforest and Eucalypt-dominated wet sclerophyll

803 forest within the Lake Vera catchment.
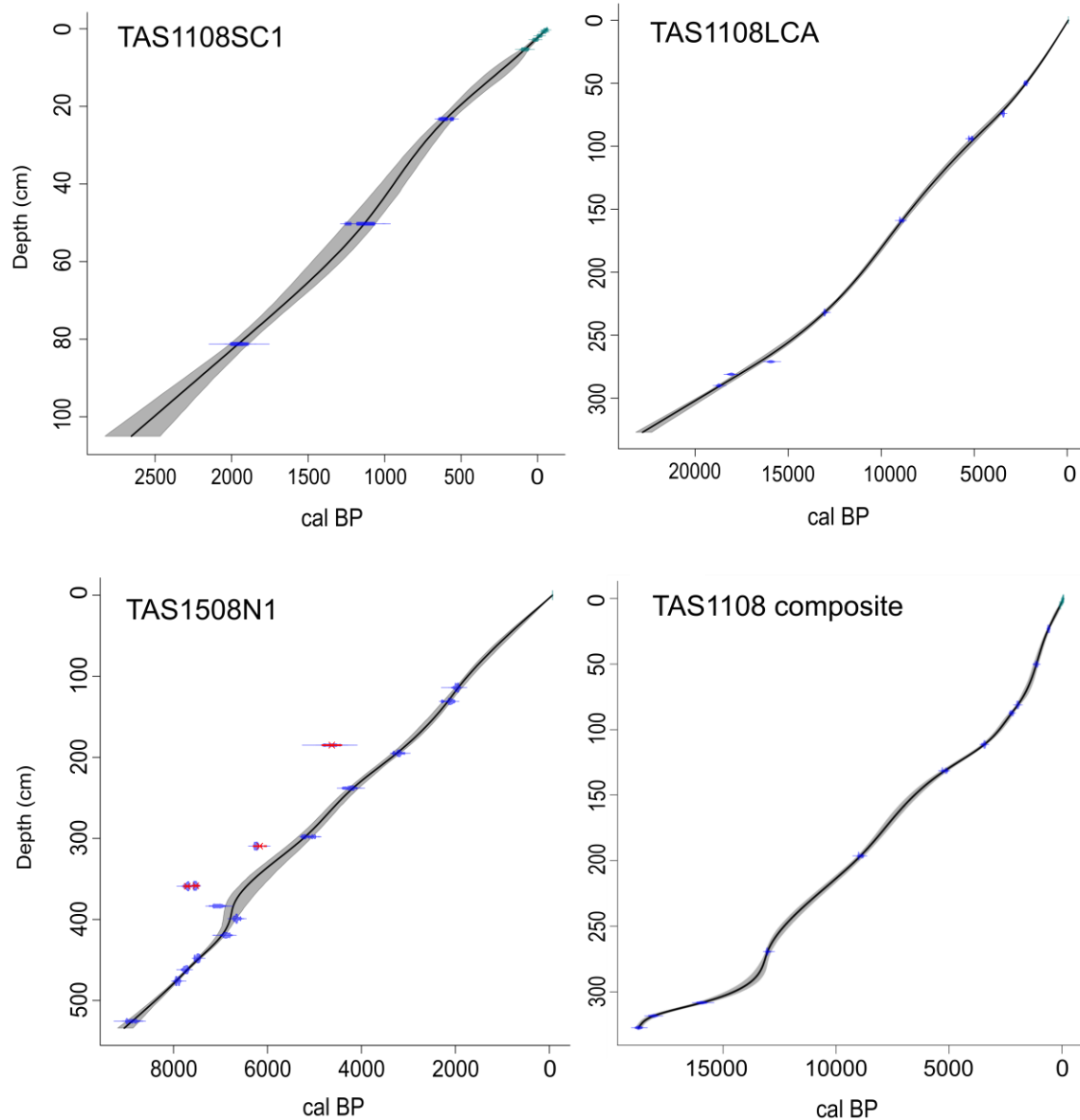
804

805 **Fig. 2** Age-depth models for all sediment sequences collected from Lake Vera. Top three panels

806 depict isolated sequences for the individual cores TAS1108SC1, TAS1108LCA and

807 TAS1508N1. TAS1108SC1 plots ^{14}C combined with CIC (Constant Initial Concentration) ^{210}Pb

808 ages in the dated sequence. Main (bottom) panel depicts the age-depth model constructed for

809 the composite core (TAS1108SC1 and TAS1108LCA). Plotted depths are adjusted composite

810 depths, rather than original. ^{14}C dates were calibrated using the Southern Hemisphere

811 calibration curve (Hogg et al. 2013) and the *clam v2.2* software package was used to perform

812 the age-depth modelling (Blaauw 2010).

813

814

815
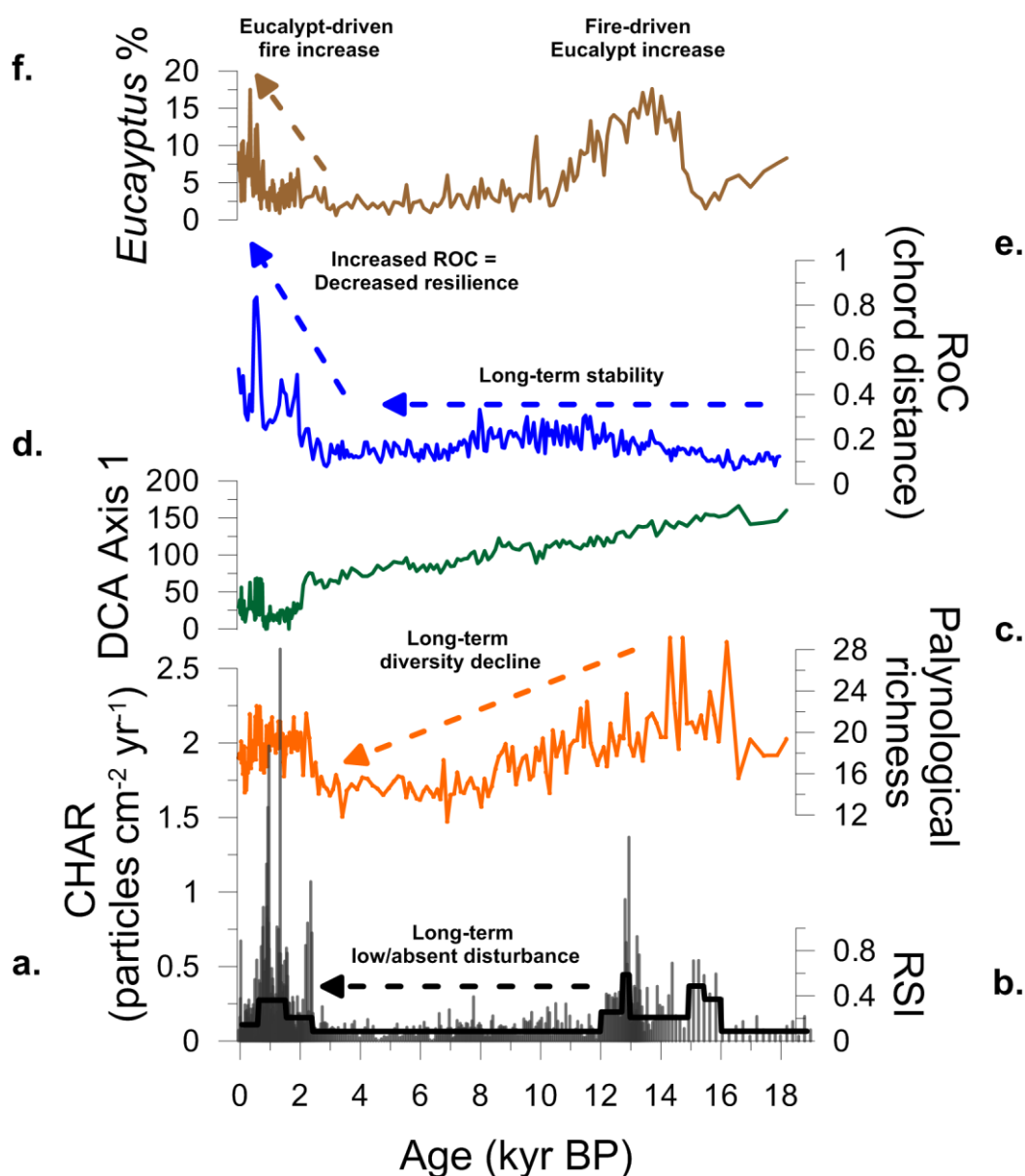
Fig. 3 Pollen, spore and charcoal data for Lake Vera. All data are in percent values (excluding
macroscopic CHAR). Zones are based on the results of a stratigraphically constrained cluster
analysis (CONISS; Grimm 1987). The composite macroscopic CHAR curve is shown. Taxa
are grouped into broad associations based on climatic niche preference or ecological response
to disturbance. Note the change in x-axis scale. Grey shaded area denotes the ACR (Pedro et
al., 2016)

822
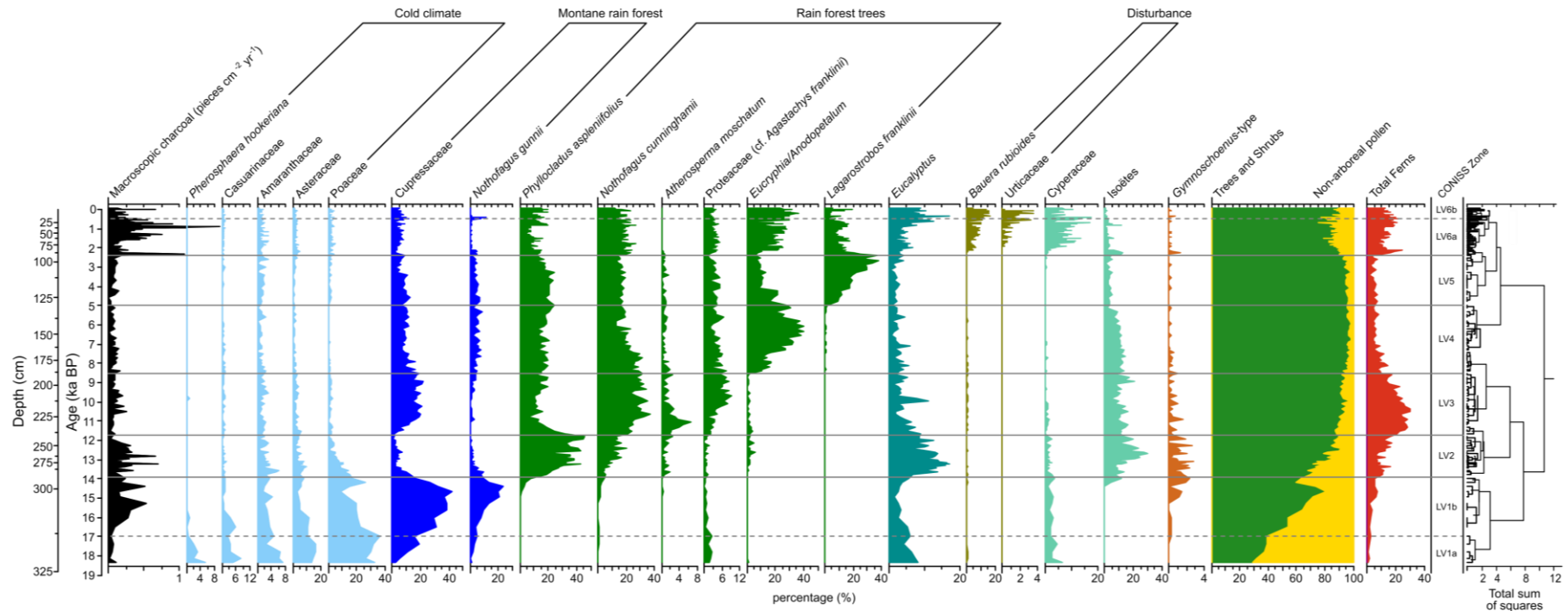
823

824 **Fig. 4** Lake Vera summary plot showing (a.) Lake Vera macroscopic CHAR; (b.) Rodoinov regime shift index (RSI) for the Lake Vera macroscopic CHAR;

825 (c.) DCA axis 1; (d.) palynological richness (species diversity); (e.) rate-of-change (RoC); (f.) *Eucalyptus* % pollen values (terrestrial pollen sum).

826

827
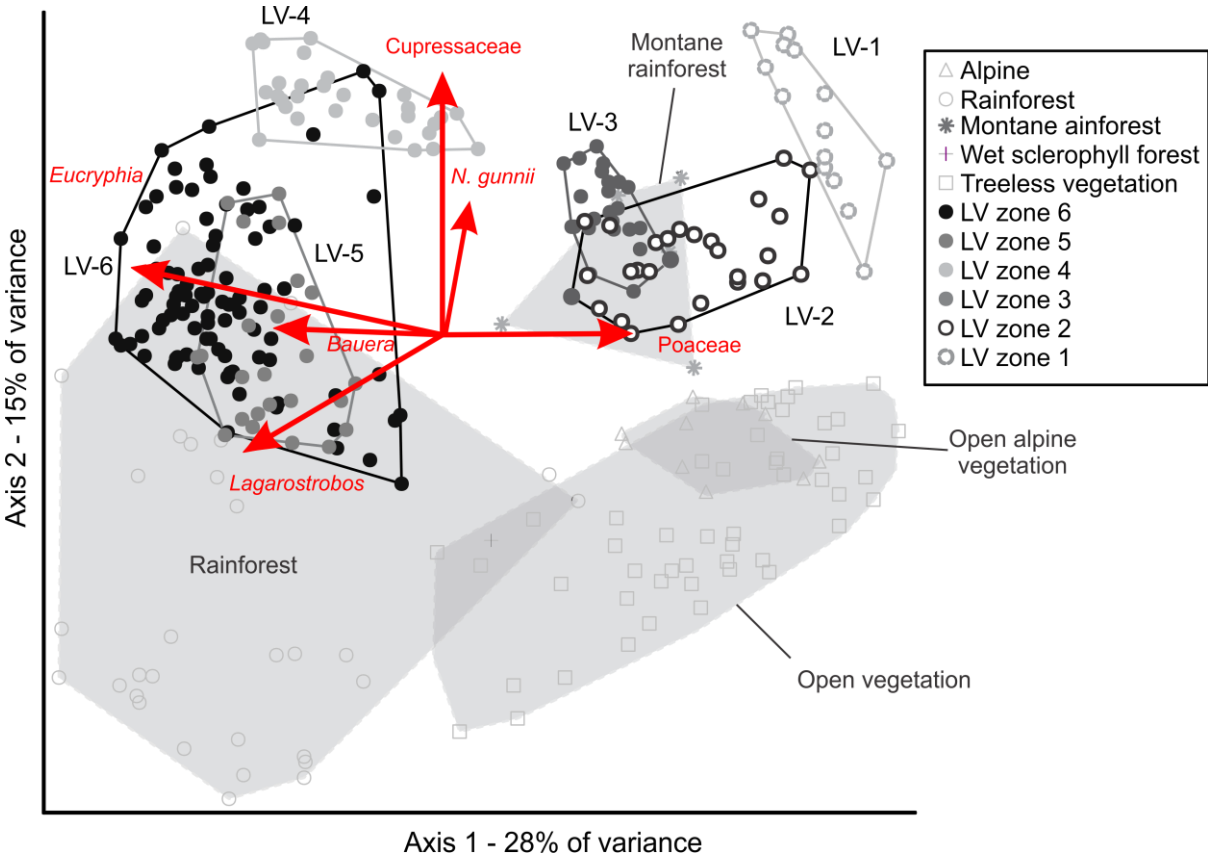
Fig. 5 DCA ordination biplot of terrestrial pollen data and the modern pollen dataset of Fletcher

and Thomas (2007). Red arrows indicate species correlations with the ordination axes above R^2

0.3. Pollen zones are derived from the pollen diagram in Fig. 4.
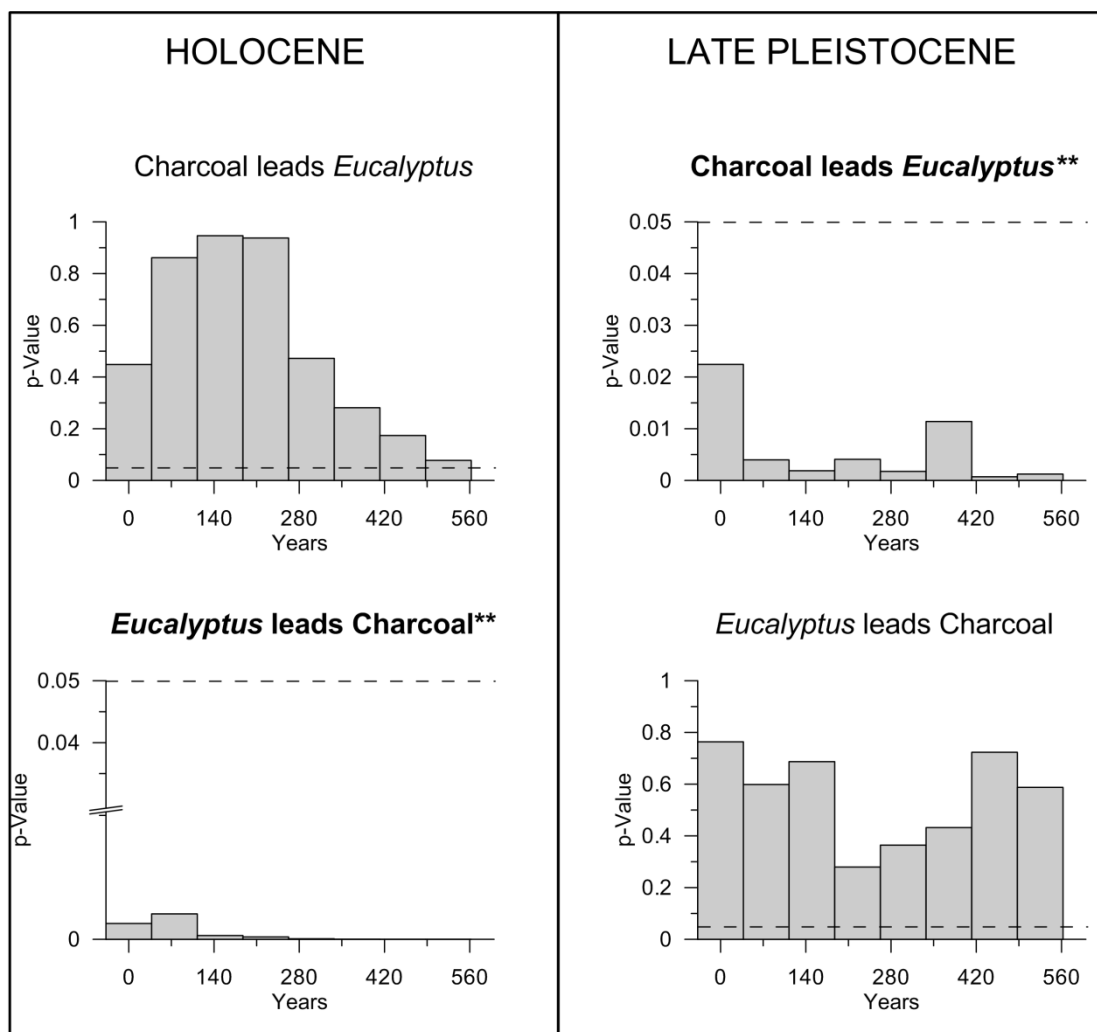
831 .

832 **Fig. 6** Results from the Granger test for causality. Two hypotheses were tested for Holocene

833 and late Pleistocene: "Charcoal leads *Eucalyptus*" (top) and "*Eucalyptus* leads charcoal"

834 (bottom). Significance level: 95%.
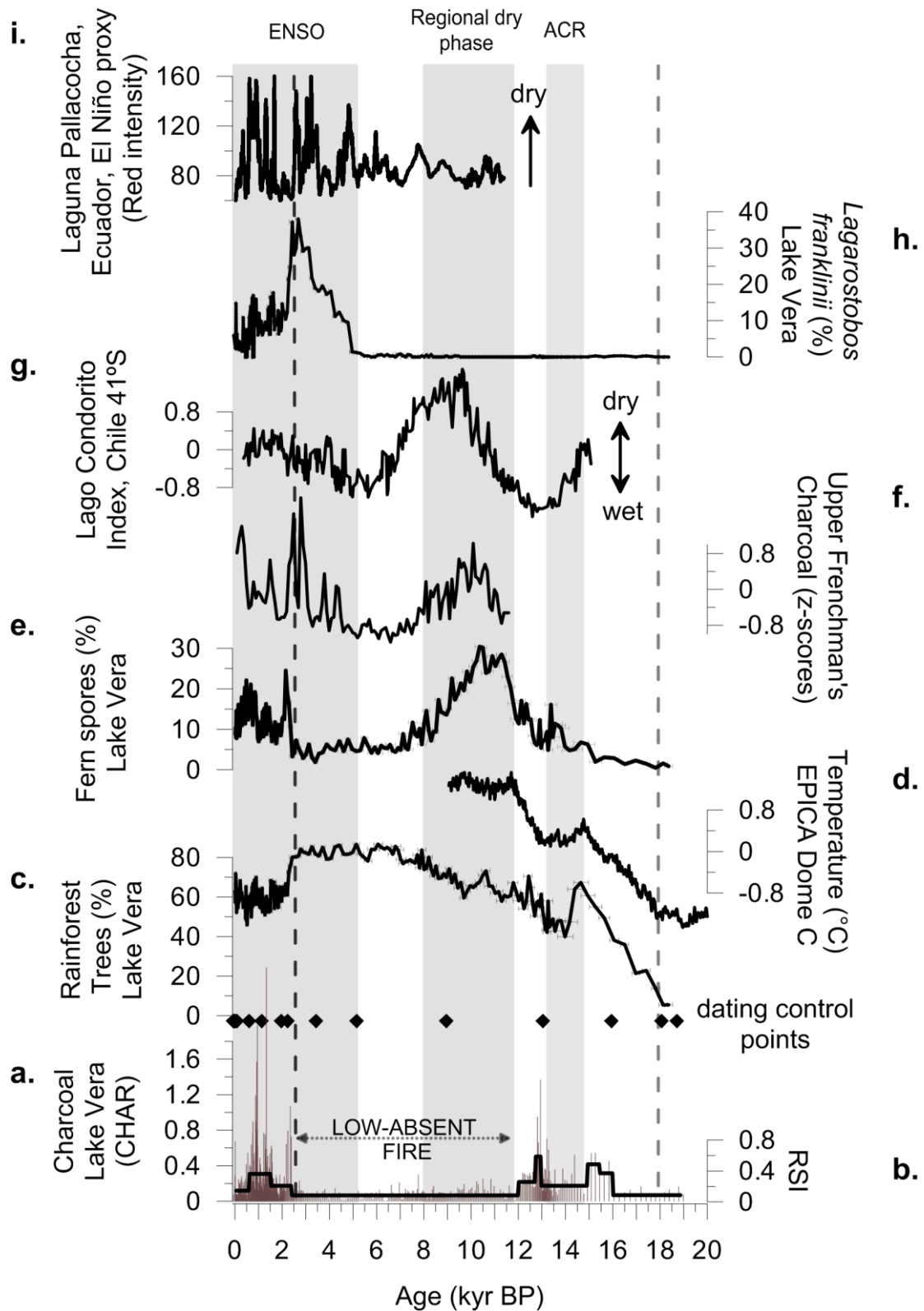
Fig. 7 Summary plot showing (a.) Lake Vera macroscopic CHAR; (b.) Rodoinov regime shift

index for the Lake Vera macroscopic CHAR; (c.) Lake Vera rainforest trees (percent terrestrial

pollen sum); (d.) composite stack of Antarctic ice core d18O (temperature proxy); (e.) Lake

839   Vera fern spores (percent terrestrial pollen sum); (f.) Upper Frenchman's Cap macroscopic

840   CHAR composite (Lake Gwendolyn and Lake Nancy) (Fletcher et al. 2015); (g.) Lago

841   Condorito North Patagonian Forest Index (SWW-derived moisture proxy) from 41°S in Chile

842   (Moreno 2004); (h.) Lake Vera *Lagarostrobos franklinii* pollen (percent terrestrial pollen sum);

843   (i.) Laguna Pallcacocha, Ecuador, red intensity (El Niño proxy), an erosion proxy tracking

844   sediment deposition associated with El Niño rainfall in Ecuador (Moy et al. 2002). Grey shaded

845   bars correspond to climate phases discussed in the text. ACR – Antarctic Cold Reversal, ENSO

846   – El Niño Southern Oscillation. Black diamonds indicate the location of dating controls. Error

847   bars on Lake Vera data show age uncertainty produced from age-depth modeling. Arrows and

848   text describe the climate inference derived from the proxy data. Vertical dashed line shows the

849   termination of the Last Glacial Maximum (Schaefer et al. 2006).

850